Thermomechanical Behaviors of Shape Memory Alloy Thin Films and Their Application

Jin-Ho Roh* and In Lee**
Department of Aerospace Engineering,
Korea Advanced Institute of Science and Technology, 373-1 Guseong-dong,
Yuseong-gu, Daejeon, Korea 305-701

Abstract

The thermomechanical behaviors of SMA thin film actuator and their application are investigated. The numerical algorithm of the 2-D SMA thermomechanical constitutive equation is developed and implemented into the ABAQUS finite element program by using the user defined material (UMAT) subroutine. To verify the numerical algorithm of SMAs, the results are compared with experimental data. For the application of SMA thin film actuator, the methodology to maintain the precise configuration of inflatable membrane structure is demonstrated.

Key Word : Thermomechanical Behavior, Shape Memory Alloys, Finite Element Method, Inflatable Membrane Structure

Introduction

Shape memory alloys (SMAs) offer a combination of novel properties, such as shape memory effect, pseudoelasticity, biocompatibility and high damping capacity, which enable them to be widely used in biomedical, micro-electro-mechanical systems (MEMS), and aerospace engineering [1-4]. Especially, when the SMA thin film type actuator is used in micro actuator, it has the following advantages, 1) low driving voltage 2) large force per volume and weight 3) faster response compared with bulk SMA actuator [5]. For this reason, SMA becomes excellent candidates for micro actuators when fabricated as thin films. But the very complicated thermomechanical behaviors make it difficult to apply SMAs for micro actuator or machine. So, appropriate numerical modeling and simulation tools are needed to support design, performance evaluation, and standardization of SMA actuator.

In this research, the thermomechanical behaviors of SMA thin film associated with stress-induced and temperature-induced transformation are investigated. The numerical algorithm of the 2-D SMA thermomechanical constitutive equation is developed and implemented into the ABAQUS finite element program by using user defined material (UMAT) subroutine to analyze the unique characteristics of SMA thin film. The thermomechanical behavior of SMA thin film is numerically investigated and the result is compared with experiment. For the application of SMA thin film actuator, the methodology to maintain the precise configuration of inflatable membrane structure is demonstrated.

Numerical Algorithm of Shape Memory Alloy Thin Film

For the numerical analysis, the 2-D incremental formulation of the SMA constitutive model is developed to predict the thermomechanical responses of SMA thin film. For 2-D problems, the

* Post-doctoral Researcher
** Professor, President of KSAS, Associate Fellow of AIAA, and Member of the Korean Academy of Science and Technology
E-mail : inlee@asdl.kaist.ac.kr Tel : 042-869-3717 Fax : 042-869-3710

general expressions derived in Lagoudas model [6] have to be modified. The model consists of three sets of equations: i) the constitutive equation, ii) the transformation equation, and iii) the transformation surface equation. The constitutive equation can be expressed as describing the increment of strain, $\dot{\epsilon}$, in terms of the increments of stress, $\dot{\sigma}$, temperature, $\dot{T}$, and martensite fraction, $\dot{\xi}$, i.e.,

$$\dot{\epsilon} = S\dot{\sigma} + \alpha\dot{T} + Q\dot{\xi} \tag{1}$$

where, $S = C^{-1}$ is the elastic compliance matrix, α is the thermal expansion coefficient vector. The stress, strain, thermal expansion, and compliance matrix can be expressed as the condition of plane stress.

$$\sigma = [\sigma_{xx}, \sigma_{yy}, \sigma_{xy}]^T, \epsilon = [\epsilon_{xx}, \epsilon_{yy}, \epsilon_{xy}]^T, \alpha = [\alpha_{xx}, \alpha_{yy}, 0]^T,$$

$$S = \begin{bmatrix} 1/E & -\nu/E & 0 \\ -\nu/E & 1/E & 0 \\ 0 & 0 & 2(1+\nu)/E \end{bmatrix} \tag{2}$$

The other term in Eq. 1 is defined by,

$$Q = \Delta S\sigma + \Delta\alpha(T - T_o) + \Lambda \tag{3}$$

The prefix Δ in Eq. 3 indicates the difference of a quantity between the martensite and austenite phases as follows:

$$\Delta S = S^M - S^A, \Delta\alpha = \alpha^M - \alpha^A \tag{4}$$

The superscript A stands for austenite phase, and superscript M stands for the martensite phase. Λ is the transformation strain direction and is assumed to have the following form:

$$\Lambda = \begin{cases} \dfrac{H}{2\bar{\sigma}^{eff}}[(2\sigma_{xx} - \sigma_{yy}), (-\sigma_{xx} + 2\sigma_{yy}), 3\sigma_{xy}]^T & , \dot{\xi} > 0 \\ \dfrac{H}{\bar{\epsilon}^{t-r}}[\epsilon_{xx}^{t-r}, \epsilon_{yy}^{t-r}, \epsilon_{xy}^{t-r}] & \dot{\xi} < 0 \end{cases} \tag{5}$$

where H is the maximum uniaxial transformation strain, ϵ^{t-r} is the transformation strain at the reversal of phase transformation, and

$$\bar{\sigma}^{eff} = \sqrt{\sigma_{xx}^2 + \sigma_{yy}^2 - \sigma_{xx}\sigma_{yy} + 3\sigma_{xy}^2}, \ \bar{\epsilon}^{t-r} = \sqrt{\frac{2}{3}\epsilon^{t-r} \cdot \epsilon^{t-r}} \tag{6}$$

The transformation equation, which relates the increment of martensite fraction to transformation strain, $\bar{\epsilon}^t$, i.e.,

$$\dot{\bar{\epsilon}}^t = \Lambda\dot{\xi} \tag{7}$$

and the transformation surface equation, which controls the start of the forward and reverse phase transformation, i.e.,

$$\begin{aligned} \pi = {} & \sigma\Lambda + \frac{1}{2}\Delta\alpha\sigma(T - T_o) \\ & + \rho\Delta c\left[(T - T_o) - T\ln\left(\frac{T}{T_o}\right)\right] + \rho\Delta s_o T - \frac{\partial f}{\partial\xi} - \rho\Delta u_o = \pm Y^* \end{aligned} \tag{8}$$

where π is the thermodynamic force conjugated to ξ. Also, ρ, c, s_o, and u_o are the mass density, specific heat, specific entropy, specific internal energy at the reference state, respectively. The plus sign on the right hand side in Eq. 8 should be used for the forward phase transformation (austenite

to martensite), while the minus sign should be used for the reverse transformation (martensite to austenite). Note that the material constant Y^* is the measure of internal dissipation due to phase transformation and can be interpreted as the threshold value of the transformation surface π for the start of the phase transformation.

The transformation function can be defined in terms of the transformation surface equation as follows:

$$\Phi = \begin{cases} \pi - Y^*, & \dot{\xi} > 0 \\ -\pi - Y^*, & \dot{\xi} < 0 \end{cases} \tag{9}$$

The transformation function Φ takes a similar role to the yield function in plasticity theory, but in this case, an additional constraint for martensite fraction ξ must also be satisfied. Constraints on the evolution of the martensite fraction are expressed as,

$$\dot{\xi} \geq 0,\ \Phi(\sigma, T, \xi) \leq 0,\ \Phi\dot{\xi} = 0 \tag{10}$$

$$\dot{\xi} \leq 0,\ \Phi(\sigma, T, \xi) \leq 0,\ \Phi\dot{\xi} = 0$$

The inequality constraints on $\Phi(\sigma, T, \xi)$ is called as the transformation condition and regarded as a constraint on the state variables' admissibility. For $\Phi < 0$, Eq. 10 requires $\dot{\xi} = 0$ and elastic response is obtained. On the other hand, the forward-phase transformation (austensite to martensite) is characterized by $\Phi = 0$ and $\dot{\xi} > 0$, while the reverse-phase transformation (martensite to austenite) is characterized by $\Phi = 0$ and $\dot{\xi} < 0$.

In the numerical implementing of the SMA constitutive model, the tangent stiffness and the stress at each integration point of all elements should be updated in each iteration for given increments of strain and temperature. The the relationship between stress increments and strain and temperature increments can be expressed by,

$$\dot{\sigma} = L\dot{\epsilon} + l\dot{T} \tag{11}$$

where the tangent stiffness L and tangent thermal moduli l are defined by,

$$L = \left(S - \frac{Q \times \frac{\partial \Phi}{\partial \sigma}}{\frac{\partial \Phi}{\partial \xi}} \right)^{-1}, \quad l = S^{-1} \times \left(Q \cdot \frac{\frac{\partial \Phi}{\partial T} - \frac{\partial \Phi}{\partial \sigma} \times S^{-1} \times \alpha}{\frac{\partial \Phi}{\partial \xi} - \frac{\partial \Phi}{\partial \sigma} \times S^{-1} \times Q} - \alpha \right) \tag{12}$$

To calculate the increment of stress for given strain and temperature increments, Newton-Raphson iteration method has been used. For the numerical results of SMA thin film, the ABAQUS finite element program has been utilized with user material (UMAT) subroutine[4,6].

Thermomechanical Behaviors of Shape Memory Alloy Thin Film

The numerical results of thermomechanical behaviors of SMA thin film are compared with experimental results of Lexcellent et al. [7]. The dimension of the SMA thin film specimen is 1mm (width) × 5mm (length) × 0.006mm (thickness). For the numerical model of SMA, 10×4 membrane elements (M3D4) supported by ABAQUS are used. Thermomechanical properties of SMA thin film measured by experiment are shown in Table 1 [7]. The critical stresses and the stress influence coefficients $\left(\frac{d\sigma}{dT}\right)^M$ and $\left(\frac{d\sigma}{dT}\right)^A$ of the SMA thin film are presented in Fig. 1. As can be seen, the stress influence coefficients are different for forward and reverse phase transformation. However, Lagoudas [6] just derived equation and simulate in case of $\left(\frac{d\sigma}{dT}\right)^M = \left(\frac{d\sigma}{dT}\right)^A$.

Table 1. Material properties of SMA thin film

Moduli, Poisson's ratio, Thermal expansion	Transformation temperatures	Transformation constants	Maximum transformation strain
$E^A = 40.0 \times 10^9 Pa$ $E^M = 30.0 \times 10^9 Pa$ $\nu^A = \nu^M = 0.34$ $\alpha^A = 22 \times 10^{-6}/K$ $\alpha^M = 10 \times 10^{-6}/K$	$A^{of} = 321.0K$ $A^{os} = 312.0K$ $M^{os} = 240.0K$ $M^{of} = 218.0K$	$\left(\frac{d\sigma}{dT}\right)^A = 13.845 \times 10^6 Pa/(m^3 K)$ $\left(\frac{d\sigma}{dT}\right)^M = 4.212 \times 10^6 Pa/(m^3 K)$	$H = 0.04$

So, new concept strain hardening parameters are proposed in this research. The effective specific entropy difference is suggested differently in case of forward and reverse phase transformation as follows:

$$\Delta s_o^A = -\frac{H}{\rho}\left(\frac{d\sigma}{dT}\right)^A,$$

$$\Delta s_o^M = -\frac{H}{\rho}\left(\frac{d\sigma}{dT}\right)^M \tag{13}$$

Based on the Eq. 13, transformation strain hardening material constants can be derived such as follows:

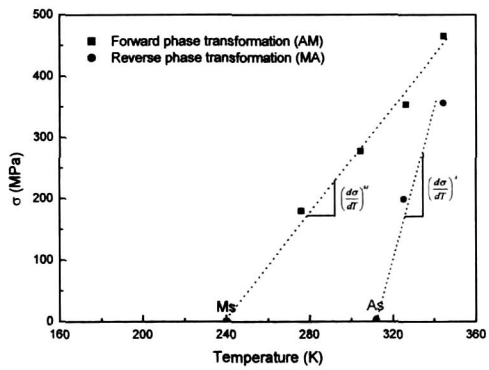

Fig. 1. The temperature dependence of critical stress for inducing forward transformation and reverse transformation

$$\gamma = \frac{1}{2}\rho\left(\Delta s_o^M M^{os} + \Delta s_o^A A^{of}\right),$$
$$\rho b^A = -\rho\Delta s_o^A\left(A^{of} - A^{os}\right),\ \rho b^M = -\rho\Delta s_o^M\left(M^{os} - M^{of}\right) \tag{14}$$

Also, the measure of internal dissipation due to phase transformation, Y^*, can be induced.

$$Y^* = -\frac{1}{2}\rho\Delta s_o^A \times A^{of} + \frac{1}{2}\rho\Delta s_o^M \times M^{os} + \frac{1}{4}\rho\Delta s_o^M\left(M^{os} - M^{of}\right) - \frac{1}{4}\rho\Delta s_o^A\left(A^{of} - A^{os}\right) \tag{15}$$

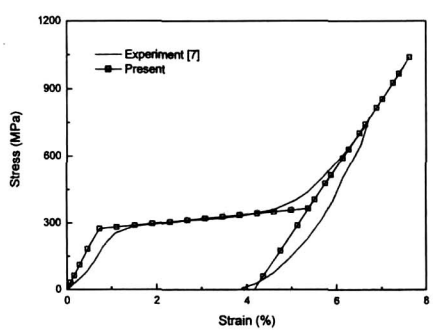

(a) Temperature=305K

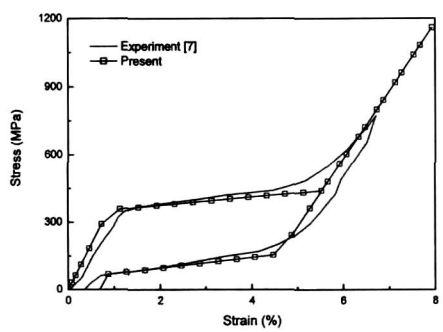

(b) Temperature=325K

Fig. 2. The stress-strain curves with various temperatures

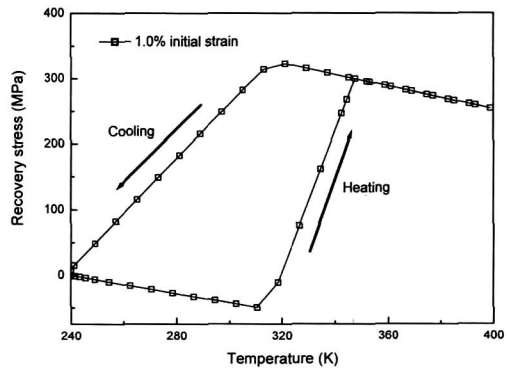

Fig. 3. Hysteresis of recovery stress with thermal cycle

The simple uniaxial stress-strain curves with various temperatures are investigated and the results are compared with experimental results. In Fig. 2, there are very good agreements between numerical and experimental results.

To estimate the performance of SMA thin film actuator, the hysteresis loop of recovery stress with respect to temperature variation is investigated in Fig. 3. SMA strip is restrained during the phase transformation induced by heating process, so that the large recovery stress is generated by shape memory effect.

Inflatable Strut with SMA Thin Film

Inflatable membrane structures are faced with many challenges, particularly the need to achieve and maintain precise shape. So, the reliable maintenance of the shape or surface precision during the mission life is one of the most important technologies for the development of inflatable structures. In this section, the methodology to correct local deviations in the shape of the inflatable membrane structures with SMA thin film actuator is numerically demonstrated.

The inflatable antenna is comprised of two basic structures: the inflatable reflector assembly and torus / strut supporting structure (Fig. 4). For the demonstrations of surface configuration control, the inflatable strut with SMA thin film is proposed. The numerical model of membrane inflatable strut with SMA thin film is illustrated in Fig. 5.

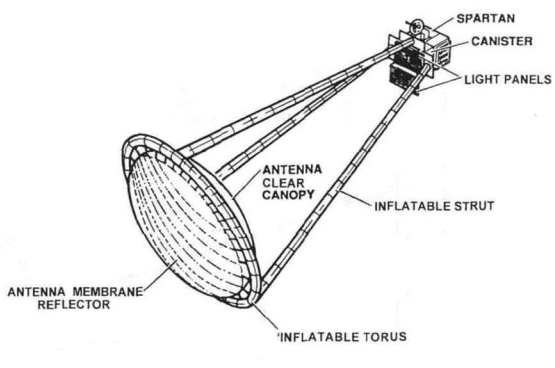

Fig. 4. Inflatable antenna configuration

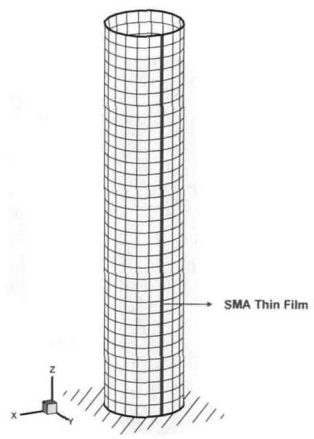

Fig. 5. Inflatable strut with SMA thin film

Table 2. Geometric and material properties of inflatable strut

Modulus (E)	$2.5GPa$
Poisson's ratio (ν)	0.34
Coefficient of Thermal Expansion (α)	$20\times10^{-6}/^{o}C$
Thickness (t)	$25\times10^{-6}m$
Length (L)	$0.95m$
Diameter (D)	$0.19m$

The host membrane structure and SMA thin film are numerically modeled using 693 and 33 membrane elements (M3D4) supplied by ABAQUS finite element program, respectively. To consider the nonlinear behaviors of inflated membrane structures, the wrinkling algorithm is applied [8]. Thin film SMA with width of $6mm$ is adhered on surface of the structure. The thermomechanical properties of SMA thin film are used from Table 1. The inflatable strut is made of Kapton film and geometric and material properties are illustrated in Table 2. SMA thin film has initial strain in the z-direction. When SMA thin film is activated by raising its temperature above the austenite start temperature, strain recovery in the activated SMA thin film causes the structure bending due to the off-center placement of the SMA thin film.

The maintenance of precise shape configuration under thermal environment is investigated to show the effectiveness of SMA thin film actuator. It is assumed that the surface where SMA thin film is adhered is subjected to thermal load of $60^{o}C$ due to solar radiation. But the opposite surface is subjected to thermal load of $-80^{o}C$ due to shadow area. The temperature distribution of inflatable strut is illustrated in Fig. 6. The internal pressure of $3{,}447Pa$ $(0.5psi)$ is applied. As can be seen from Fig. 7, the tip deflection without SMA thin film is decreased due to temperature difference. However, in case with SMA thin film, tip deflection should tend to recover from thermally deformed position to the initial state after temperature of $40^{o}C$ which is the nearly austenite start temperature $(A^{os}=39^{o}C)$ of SMA thin film (Table 1). When 0.5% initial strain is subjected, tip deflection is increased at temperature of nearly $39^{o}C$ and decreased again due to thermal expansion effect after when temperature-induced phase transformation is completed. In case of 1% initial strain of SMA thin film, the deformed shape configuration is almost recovered to original state and the magnitude deformation of inflatable strut at temperature of $60^{o}C$ is illustrated in Fig. 8. As can be seen, deformation is concentrated near the area on which SMA thin film is adhered. Also, it can be found that the wrinkling area is developed from Fig. 9. By using SMA thin film with 1% initial strain, the maintenance of shape configuration of inflatable

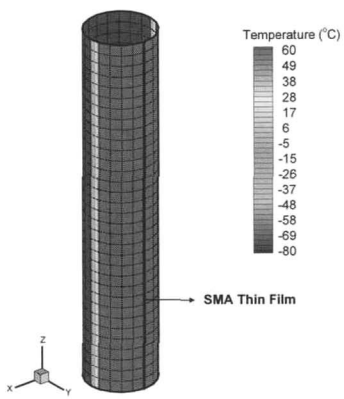

Fig. 6. Temperature distribution of inflatable strut

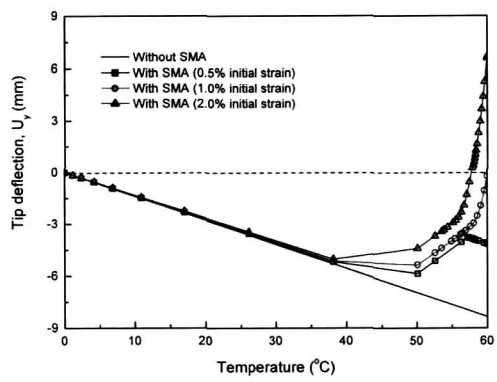

Fig. 7. Shape maintenance effect of SMA thin film

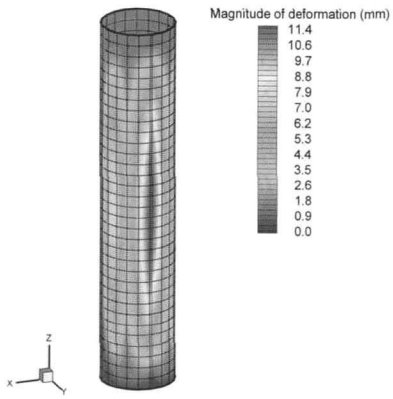

Fig. 8. The deformation of inflatable strut at temperature of $60^{o}C$

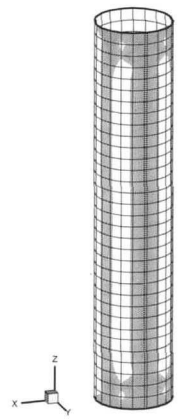

Fig. 9. Wrinkling area of inflatable strut at temperature of $60^{o}C$

strut could be possible. But the negative effects on the structure are also combined due to recovery stress and strain of SMA thin film: i) the deformation is locally concentrated and ii) wrinkling area is developed. In case of 2% initial strain, the tip deflection is excessively offset from original state due to excessive recovery strain or displacement of SMA thin film. Such excessively offset is induced by recovery strain of SMA thin film depending on internal pressure of the membrane structure. So, the optimal design process is needed for the accurate position control and structural performance by determining recovery strain of SMA thin film depending on internal pressure or environmental temperature difference.

Conclusions

Thermomechanical behaviors of shape memory alloy (SMA) thin film are investigated. The numerical algorithm of the 2-D SMA thermomechanical constitutive equation is developed and implemented into the ABAQUS finite element program by using user defined material (UMAT) subroutine. For the 2-D problems, the general expression derived in Lagoudas model is modified as plane stress condition. New concept parameters related with thermodynamic energy equation are introduced to describe the specific behaviors of SMA thin film. For the verification of present developed numerical algorithm of SMA thin film, experimental results are compared with simulation. There are very good agreements between numerical and experimental results.

The methodology to maintain the precise configuration of inflatable space structure is numerically demonstrated for the application of SMA thin film actuator. It is found that thin film of SMA is very effective to control the deflection position and surface configuration from the numerical results. However, negative effects such as offset form initial configuration or wrinkled area development are induced by excessive recovery strain or displacement of SMA thin film. So, the optimal design process is needed for the accurate position control and surface configuration.

Acknowledgments

This work was supported by the Brain Korea 21 Project in 2006.

References

1. Roh, J.-H., Oh, I. K., Yang, S. M., Han, J.-H., and Lee, I., 2004, "Thermal Post-Buckling Analysis of Shape Memory Alloy Hybrid Composite Shell Panels", *Smart Materials and*

Structures., Vol. 13, pp. 1345-1350.

2. Roh, J.-H., Han, J.-H., and Lee, I., 2004, "Effect of Shape Memory Alloys on Structural Modification", *Key Engineering Materials*, Vol. 270-273, pp. 2193-2198.

3. Lee, I., Roh, J.-H., Yang, S. M., and Han, J.-H., 2005, "Shape and Vibration Control of Smart Composite Structures", *Advanced Composite Materials*, Vol. 14, pp. 121-130

4. Roh, J.-H., Han, J.-H., and Lee, I., 2006, "Nonlinear Finite Element Simulation of Shape Adaptive Structures with SMA Strip Actuator", *Journal of Intelligent Material, Systems and Structures*, To be published.

5. Shin, D. D., Mohanchandra, K. P., and Carman, G. P., 2004, "High Frequency Actuation of Thin Film NiTi", *Sensors and Actuators A: Physical*, Vol. 111, pp. 166-171.

6. Qidwai, M. A., and Lagoudas, D. C., 2000 "Numerical Implementation of a Shape Memory Alloy Thermomechanical Constitutive Model Using Return Mapping Algorithms", *International Journal for Numerical Methods in Engineering*, Vol. 47, pp. 1123-1168.

7. Lexcellent, C., Moyne, S., Ishida, A., and Miyazaki, S., 1998, "Deformation Behavior Associated with the Stress-Induced Martensitic Transformation in Ti-Ni Thin Films and Their Thermodynamic Modeling", *Thin Solid Films*, Vol. 324, pp. 184-189.

8. Roh, J.-H., Yoo, E. J., Han, J.-H., Lee, I., Kang, W. G., and Yeom, C. H., 2005, "Nonlinear Analysis of Inflatable Membrane Structures with Wrinkling Effect", *Journal of the Korea Society for Aeronautical and Space Science*, Vol. 33, pp. 33-38.